Coherent population trapping at low light levels

Iyyanki V. Jyotsna and G. S. Agarwal*
School of Physics, University of Hyderabad, Hyderabad 500 134, India
(Received 10 February 1995)

A three-level lambda (Λ) system driven by two coherent fields at the Raman resonance condition evolves to a nonabsorbing eigenstate of the Hamiltonian called the coherent population trapping (CPT) state. We study the various factors dictating the dynamical evolution of the coherences and the populations to the CPT state. We demonstrate the formation of the CPT state even at low intensities, though it takes much longer to form such a state. For the case of unequal decay rates we demonstrate an interesting sharp dip in the steady-state response of the medium at the Raman resonance condition.

PACS number(s): 42.50.Gy, 42.50.Hz

I. INTRODUCTION

A three-level system with two closely spaced ground levels optically coupled to a common excited level by two coherent fields gives rise to trapping of population in a coherent superposition of the ground levels. The coherent superposition state is termed the coherent population trapping (CPT) state. This occurs under the condition that the frequency difference between the two fields is equal to the separation between the two ground levels.

Alzetta *et al.* [1] first observed nonabsorption resonances when the fluorescent light of sodium vapor illuminated by a multimode laser field was analyzed as a function of applied magnetic field. It was found that a steady decrease in fluorescence intensity occurs when some hyperfine transitions of the ground state matched the frequency difference of the two laser modes. Gray, Whitley, and Stroud, and Murnick *et al.* also reported similar experimental results [2]. Orriols [3] gave a theoretical explanation of the phenomenon using the nonlinear effects of coherence and interference due to simultaneous excitation pathways. The CPT state has been extensively studied using classical fields [3–5] and the conditions for population trapping have been explicitly derived. The effect of the various relaxation mechanisms, strength of the laser driving fields [4], bandwidths of the fields [5], etc., have been analyzed thoroughly. Recently, CPT has been dealt with in the context of quantized fields and some novel properties were discovered [6]. The CPT concept has been utilized in different situations. Some of the most prominent applications were the demonstration of lasing without inversion [7] and efficient transfer of population from one state to the other [8].

In a Λ system it is well known that the trapping state has the structure (cf. Fig. 1)

$$|\psi\rangle = -G_1|2\rangle + G_2|3\rangle \ , \tag{1}$$

where G_1 and G_2 are the Rabi frequencies of the fields acting on the transitions $|1\rangle \leftrightarrow |3\rangle$ and $|1\rangle \leftrightarrow |2\rangle$. Clearly if $G_1 = G_2$ then $\rho_{22} = \rho_{33} = \frac{1}{2}$ irrespective of the values of G_1 and G_2. Thus G_1 and G_2 can be arbitrarily small and yet the trapping state will be formed. This is somewhat against one's intuition based on the perturbation theory which would imply that only a small amount of population can be transferred for weak fields. It is clearly important to understand the dynamics of the system leading to the formation of trapping states at low intensities.

In this paper we address some of the dynamical questions. In particular we study how the CPT state is formed and how the evolution depends on different parameters. An important point which emerges from this study is that the CPT state is produced *irrespective* of the strength of the applied fields. Another feature observed is that with decreasing fields it takes longer and longer to form the CPT state. Thus the CPT state can only be obtained from a nonperturbative analysis. The organization of the paper is as follows.

In Sec. II we introduce the model and use the density-matrix formalism to study the dynamical evolution to the CPT state. We predict interesting effects of laser field strength and spontaneous decay rate on the time scales of evolution. In Sec. III we exhibit an unusually sharp dip for Λ systems with two unequal decay rates. Note that in most Λ systems such as in Cs and Rb one will encounter unequal decay rates. Note further that unequal decays play an important role in the context of lasing without inversion [9]. In Sec. IV we summarize the main conclusions of the paper and point out the possibility of the effect of a dense medium [10] on the dynamics of the system.

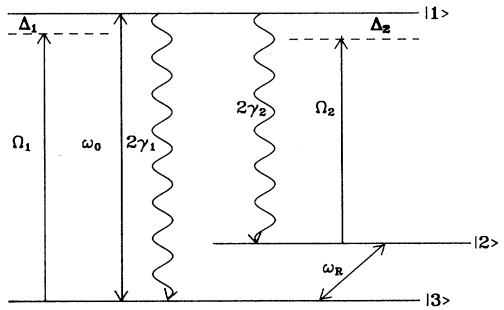

FIG. 1. Schematic representation of a three-level Λ system.

*Present address: Physical Research Laboratory, Navrangpura, Ahmedabad 380 009, India. Electronic address: gsa@prl.ernet.in

II. THE MODEL AND DYNAMICAL EVOLUTION TO THE CPT STATE

Consider a three-level system consisting of a single resonant excited state $|1\rangle$ optically coupled with two closely spaced ground sublevels $|2\rangle$ and $|3\rangle$. States $|1\rangle$ and $|2\rangle$ have energies $\hbar\omega_0$ and $\hbar\omega_R$ with respect to the state $|3\rangle$. Two classical monochromatic fields of frequencies Ω_1 and Ω_2 couple the transitions $|1\rangle\leftrightarrow|3\rangle$ and $|1\rangle\leftrightarrow|2\rangle$, respectively. The states $|2\rangle$ and $|3\rangle$ are not coupled directly due to parity constraints. Let $2\gamma_1$ ($2\gamma_2$) be the spontaneous emission rate from state $|1\rangle$ to state $|3\rangle$ ($|2\rangle$) (Fig. 1).

The total Hamiltonian of the system [11] is written as

$$H=\hbar\omega_0 A_{11}+\hbar\omega_R A_{22}-\vec{d}_{13}\cdot\vec{E}_1 A_{13}\exp(-i\Omega_1 t) -\vec{d}_{12}\cdot\vec{E}_2 A_{12}\exp(-i\Omega_2 t)+\text{H.c.}\ , \quad (2)$$

where A_{xy} are the atomic transition operators $|x\rangle\langle y|$. Here $\vec{d}_{13}$ ($\vec{d}_{12}$) is the atomic dipole interaction term between the states $|1\rangle$ and $|3\rangle$ ($|2\rangle$) and $\vec{E}_1$ and $\vec{E}_2$ are the electric-field amplitudes. Defining $G_1=\vec{d}_{13}\cdot\vec{E}_1/\hbar$ and $G_2=\vec{d}_{12}\cdot\vec{E}_2/\hbar$ the Hamiltonian in (2) is rewritten as

$$H=\hbar\omega_0 A_{11}+\hbar\omega_R A_{22}-\hbar G_1\exp(-i\Omega_1 t)A_{13} -\hbar G_2\exp(-i\Omega_2 t)A_{12}+\text{H.c.} \quad (3)$$

The system is studied using the density-matrix formalism. The evolution of the reduced density matrix ρ for the atomic system alone is described by the Liouville equation, modified to include damping effects [12], which is given by

$$\frac{\partial\rho}{\partial t}=\frac{-i}{\hbar}[H,\rho]-\gamma_1(A_{13}A_{31}\rho-2A_{31}\rho A_{13}+\rho A_{13}A_{31}) -\gamma_2(A_{12}A_{21}\rho-2A_{21}\rho A_{12}+\rho A_{12}A_{21})\ . \quad (4)$$

The equations of motion for the components of the density matrix ρ in the rotating frame can be written as

$$\dot{\rho}_{11}=-2(\gamma_1+\gamma_2)\rho_{11}+iG_1\rho_{31}+iG_2\rho_{21}+\text{c.c.}\ , \quad (5a)$$

$$\dot{\rho}_{12}=-[\gamma_1+\gamma_2-i\Delta_2]\rho_{12}+iG_1\rho_{32}+iG_2(\rho_{22}-\rho_{11})\ , \quad (5b)$$

$$\dot{\rho}_{13}=-[\gamma_1+\gamma_2-i\Delta_1]\rho_{13}+iG_2\rho_{23} +iG_1(1-2\rho_{11}-\rho_{22})\ , \quad (5c)$$

$$\dot{\rho}_{22}=2\gamma_2\rho_{11}-iG_2\rho_{21}+\text{c.c.}\ , \quad (5d)$$

$$\dot{\rho}_{23}=i(\Delta_1-\Delta_2)\rho_{23}-iG_1\rho_{21}+iG_2^*\rho_{13}\ , \quad (5e)$$

where Δ_1 and Δ_2 are the detunings defined as $\Delta_1=\Omega_1-\omega_0$ and $\Delta_2=\Omega_2-(\omega_0-\omega_R)$.

Initially, at time $t=0$, it is assumed that the atom is in the ground state and that there are no coherences, i.e., $\rho_{33}=1$, $\rho_{11}=\rho_{22}=0$, and $\rho_{ij}=0$, where $i\neq j$. To study the evolution of the system to the CPT state from the above initial conditions the set of density-matrix equations in (5) is numerically integrated using a fourth-order Runge-Kutta method. We especially concentrate on the two-photon resonance (Raman) condition $\Delta_1=\Delta_2$.

Considering the $\Delta_1=\Delta_2=0$ situation where the two external fields are exactly on resonance with the respective atomic transitions, we study the dynamical evolution to the CPT state for various field strengths and spontaneous decay rates. We specifically present the evolution of the absorption characteristic of one of the fields (say G_2), i.e., $\text{Im}(\rho_{12})$, and the population of the level $|2\rangle$, ρ_{22}. For symmetric fields, i.e., $G_1=G_2$, the steady state (relative to the decays involved) will correspond to the trapping condition if $\text{Im}(\rho_{12})=0$ and $\rho_{22}=\frac{1}{2}$. The time is scaled as $\gamma_1 t$.

We first study the dynamics for the strong-fields situation, i.e., $G_1,G_2\gg\gamma_1,\gamma_2$. For a typical case, $G_1=G_2=10$, $\gamma_1=\gamma_2=1.0$, Rabi oscillations are exhibited in the evolution of the coherence $\text{Im}(\rho_{12})$ and the population ρ_{22} (solid curves in Fig. 2 and its inset). To get an idea about the time scales involved we numerically perform an eigenvalue analysis of the 8×8 matrix in Eq. (5). For strong fields complex eigenvalues are obtained. The complete set of eigenvalues is listed here. There are two real eigenvalues -1.0 and -2.0. The complex ones are $-2.5+28.2i$, $-1.0+14.1i$, and $-1.0+14.1i$ (degeneracy) and their complex conjugates. These predict the occurrence of Rabi oscillations [13]. The real part of the complex eigenvalues is negative, indicating that the system will approach steady state.

As the field strength is lowered the eigenvalues become completely real. For the case $G_1=G_2=0.1$, $\gamma_1=\gamma_2=1.0$, the eigenvalues are -3.96, -2.02, -2.0, -1.98, -1.98, -0.01, -0.01 (degeneracy), and -0.0099. It is also observed that the lowest eigenvalue,

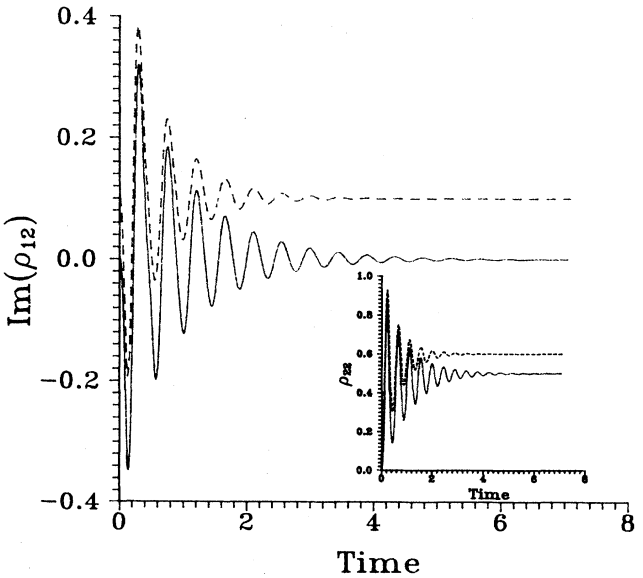

FIG. 2. Dynamical evolution of the absorption characteristic of the medium for the transition $|1\rangle\leftrightarrow|2\rangle$ with respect to field G_2, $\text{Im}(\rho_{12})$, and population of the level $|2\rangle$, ρ_{22} (inset). The time is scaled as $\gamma_1 t$. Parameters are $G_1=G_2=10,\Delta_1=\Delta_2=0$. The solid curves correspond to the decay rates $\gamma_2=\gamma_1=1.0$ and the dashed curves correspond to $\gamma_2=2$, $\gamma_1=1.0$. The dashed curves in the main figure and the inset have been shifted by 0.1 units in the positive y direction for clarity.

which dictates the time evolution to steady state, is of the order of G_1G_2. Thus the time scale at which steady state is reached is $\sim 1/G_1G_2$. For instance, when $G_1=G_2=0.1$, the time scales as $100\gamma_1 t$. This is reflected in the dynamical evolution of $\mathrm{Im}(\rho_{12})$ and ρ_{22} as depicted in Fig. 3 and its inset (solid curves). (Rabi oscillations have disappeared as the eigenvalues are real.) The steady state as observed is nothing but as given by Eq. (1). This leads to the conclusion that the CPT state is formed even at very low light levels. But, as predicted by the analysis above, as the external field strength is reduced the atomic system takes longer and longer times to reach the CPT state.

The behavior of the Λ system is also sensitive to the relative rates of spontaneous emission of the two transitions. Therefore we study the influence of the spontaneous decay rates on the evolution. We again examine the eigenvalues. For strong fields, as one of the decay rates (say γ_2) is increased from unity it is observed that the minimum eigenvalue becomes larger. In the strong-field example studied above when γ_2 is increased to 2.0 the minimum eigenvalue increases to -1.48 from -1.0 for the $\gamma_2=1.0$ case. In other words, the time taken to reach steady state (the CPT state) is relatively less. This is confirmed by the numerical integration result for the evolution shown in Fig. 2 (dashed curves). But for low fields an opposite effect occurs. As the decay rate is increased the minimum eigenvalue becomes smaller. In the low-field example studied above when γ_2 is increased to 2.0 the minimum eigenvalue reduces to -0.0066 as compared to -0.0099 for the $\gamma_2=1.0$ case. Hence it takes longer to reach steady state as confirmed from the dashed curves in Fig. 3. This is due to the buildup of a small amount of coherence ρ_{12}, which then slowly decays to zero.

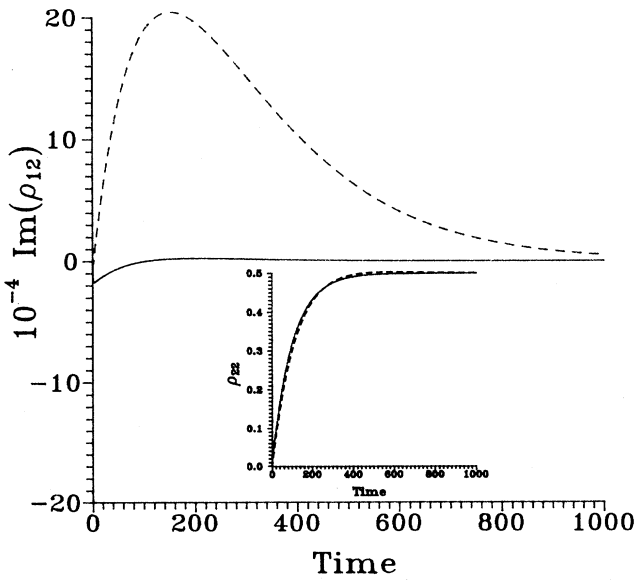

FIG. 3. Same as in Fig. 2 with parameters $G_1=G_2=0.1$, $\Delta_2=\Delta_1=0$. Solid and dashed curves correspond to $\gamma_2=\gamma_1=1.0$ and $\gamma_2=2.0$, $\gamma_1=1.0$ cases, respectively.

To understand the functional dependence of the minimum eigenvalue on the decay rates and the fields we solve for the eigenvalues of the 8×8 matrix in Eq. (5) analytically when the fields are symmetric and when $\Delta_1=\Delta_2=0$. If λ denotes the eigenvalue, then by setting $\mathrm{Det}|\rho-\lambda I|=0$ when I is an identity matrix, an eighth-order equation in λ is obtained whose roots are the eight eigenvalues. The eigenvalue equation is given as

$$(\lambda+\gamma)(\lambda^2+\lambda\gamma+2g^2)^2 [\lambda^3+3\gamma\lambda^2+(8g^2+2\gamma^2)\lambda+4g^2\gamma]=0 , \quad (6)$$

where $\gamma=\gamma_1+\gamma_2$ and $g=G_1=G_2$. The first term in Eq. (6) gives

$$\lambda=-\gamma . \quad (7)$$

This term can easily be identified in the numerical listing of the eigenvalues. The second term in Eq. (6) gives rise to a quadratic equation $\lambda^2+\lambda\gamma+2g^2=0$ whose solutions are given by

$$\lambda=\frac{-\gamma\pm\sqrt{\gamma^2-8g^2}}{2} . \quad (8)$$

For large g (strong fields), two complex conjugate roots are obtained (as found in the numerical analysis). But if g is small (low fields) two real roots occur. The roots in both these cases are repeated due to the square in the second term in Eq. (6).

The third term in Eq. (6) gives rise to a cubic equation given by

$$\lambda^3+3\gamma\lambda^2+(8g^2+2\gamma^2)\lambda+4g^2\gamma=0 . \quad (9)$$

The cubic equation accounts for the remaining three eigenvalues, one of which is the minimum. The expressions for the three eigenvalues are quite involved (not given here) and do not immediately give a clear functional dependence on the fields and the decay rates. To understand the behavior of the minimum eigenvalue in the case of low fields, we perform a perturbation calculation. Introducing the scaled parameters $\tilde{\lambda}=\lambda/\gamma$ and $\tilde{g}=g/\gamma$, Eq. (9) is transformed to

$$\tilde{\lambda}^3+3\tilde{\lambda}^2+(8\tilde{g}^2+2)\tilde{\lambda}+4\tilde{g}^2=0 . \quad (10)$$

From the numerical calculation the minimum eigenvalue is found to be of $O(\tilde{g}^2)$. So, we let $\tilde{\lambda}=\beta\tilde{g}^2$ where β is an unknown parameter which is found approximately from the perturbation calculation. In Eq. (10) the quadratic and cubic terms in $\tilde{\lambda}$ are $\sim O(\tilde{g}^4)$ and $O(\tilde{g}^6)$, respectively. The term $(8\tilde{g}^2+2)\tilde{\lambda}$ is $\sim 8O(\tilde{g}^4)+2O(\tilde{g}^2)$. As $\tilde{g}$ is quite small, retaining only the first-order terms in $\tilde{g}^2$ in Eq. (10), we get $\beta\approx -2$. Hence $\tilde{\lambda}\approx -2\tilde{g}^2$ or

$$\lambda\approx -2\frac{g^2}{\gamma} . \quad (11)$$

Thus for low fields the minimum eigenvalue approximately decreases as $2/\gamma$ with the increase in one of the decay rates. In other words the system takes a longer time to reach a steady state as was discovered in the numerical calculation above.

III. STEADY-STATE CHARACTERISTICS WITH UNEQUAL DECAY RATES

To obtain the steady-state the derivative of the density matrix ρ in Eq. (5) is set equal to zero ($\dot{\rho}=0$) and the response of the medium is evaluated as a function of the detuning Δ_2. We present the behavior of the population of state $|2\rangle$, ρ_{22}, where an interesting sharp dip is observed when there are unequal spontaneous emission rates. In the case of weak fields ($G_1, G_2 \ll \gamma_1, \gamma_2$), for instance, $G_1=G_2=0.1$ and for $\Delta_1=0$ as γ_2 is increased from being equal to γ_1 a smooth dip arises around the CPT condition ($\Delta_1=\Delta_2$) (Fig. 4). As γ_2 is increased, the height of the dip increases.

To understand the origin of the dip quantitatively the steady-state response of the system is derived analytically. For the case of symmetric fields, i.e., $G_1=G_2$, by setting $\dot{\rho}=0$ in Eq. (5) and solving the eight simultaneous linear equations a closed form for ρ_{22} is obtained. The population in level $|2\rangle$, ρ_{22}, is found to be

$$\rho_{22}=\tfrac{1}{2}+C_1+C_2 , \tag{12}$$

where

$$C_1=\frac{0.125\Delta_2^4\gamma_1^2\gamma_2-0.25\Delta_2^2G_1^2\gamma_1^2(\gamma_1+\gamma_2)}{D} , \tag{13}$$

$$C_2=\frac{0.125\Delta_2^2\gamma_1^2(\gamma_2-\gamma_1)(\gamma_1+\gamma_2)^2}{D} , \tag{14}$$

and

$$D=0.25\Delta_2^4\gamma_1^2\gamma_2+0.25\Delta_2^2\gamma_1^2(\gamma_1+\gamma_2)^3 +0.5\Delta_2^2\gamma_1^3G_1^2+G_1^4\gamma_1^2(\gamma_1+\gamma_2) . \tag{15}$$

To explicitly evaluate and compare the individual contributions of the terms C_1 and C_2, we study these as a function of Δ_2 for the case $G_1=G_2=0.1$, $\gamma_1=1.0$. As observed from Eq. (14), whenever γ_1 is equal to γ_2, C_2 disappears. From Eq. (13) it is observed that in the region $G_1<|\Delta_2|<1.0$ as Δ_2 is decreased the term with the fourth power of Δ_2 in the numerator is responsible for a decrease in C_1, even though the denominator D in Eq. (15) (having a term of the order of Δ_2^4) is also reduced simultaneously. However, in the region $|\Delta_2|<G_1$ the contribution of the fourth power of Δ_2 is negligible compared to the term with the second power of Δ_2. Hence the term C_1 is negative in the vicinity of the CPT condition. As $|\Delta_2|\to 0$ the term with the second power of Δ_2 becomes more positive and hence it leads to the small peak with a maximum of zero at $\Delta_1=\Delta_2$. The term C_1 behaves in a similar manner when γ_2 is unequal to γ_1 also. This typical behavior is depicted in the Fig. 5(a) for the case $\gamma_2=2.0$.

Once γ_2 is made unequal to γ_1, for example, the case $\gamma_2=2.0$, the term C_2 starts contributing. In the region $G_1<|\Delta_2|<1.0$, as Δ_2 is decreased, due to the presence of only a second-order term in Δ_2 in the numerator, the decrease in the denominator D in Eq. (15) increases the term C_2. However, in the region $|\Delta_2|<G_1$, the term of the order of the fourth power of G_1 is larger than the term with the fourth power of Δ_2 in the denominator D.

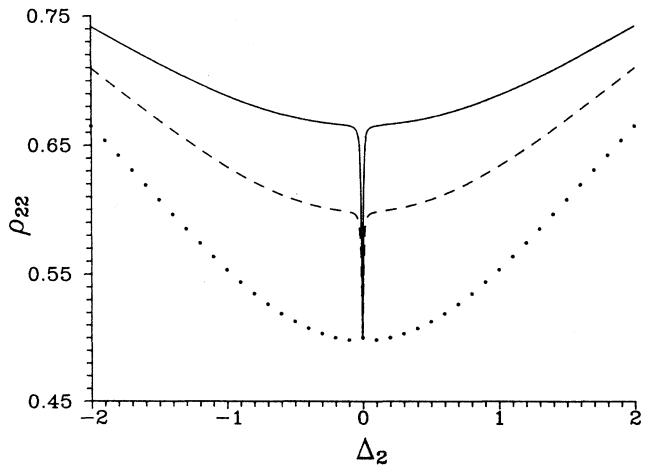

FIG. 4. The behavior of the population of level $|2\rangle$, ρ_{22}, as a function of the detuning Δ_2 for varying γ_2 values. The parameters are $G_1=G_2=0.1$, $\Delta_1=0$, $\gamma_1=1.0$. The dotted curve represents $\gamma_2=1.0$, the dashed curve $\gamma_2=1.5$, and the solid curve $\gamma_2=2.0$.

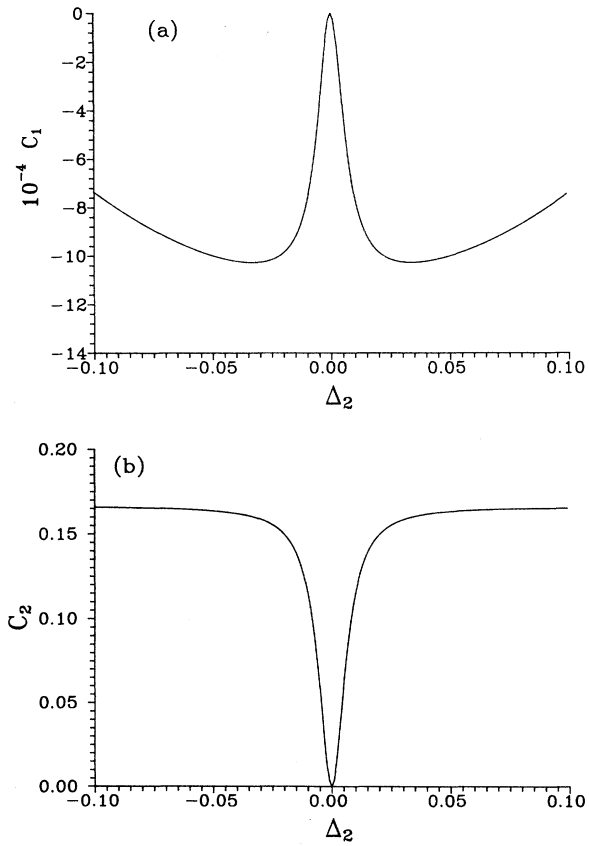

FIG. 5. The behavior of the two terms contributing to ρ_{22} as a function of the detuning Δ_2 in the region $|\Delta_2|<G_1$. (a) C_1 and (b) C_2. The parameters are $G_1=G_2=0.1$, $\Delta_2=0$, $\gamma_1=1.0$, and $\gamma_2=2.0$.

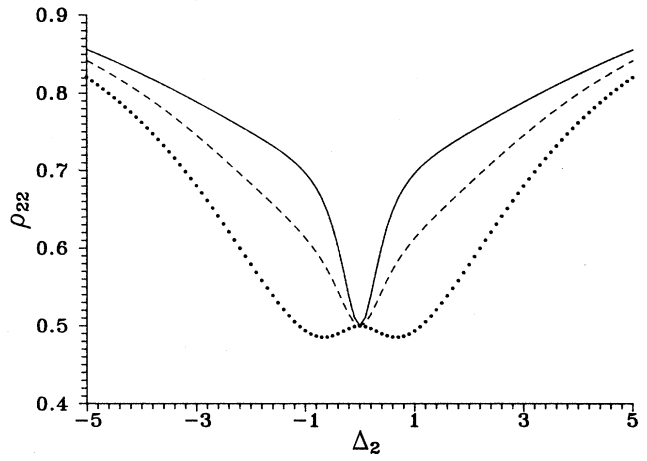

FIG. 6. Same as in Fig. 4 but with parameters $G_1=G_2=1.0$, $\Delta_1=0$, $\gamma_1=1.0$. The dotted curve represents $\gamma_2=1.5$, the dashed curve $\gamma_2=2.5$, and the solid curve $\gamma_2=3.5$.

Hence any decrease in Δ_2 results in a decrease of the numerator of C_2 without affecting the denominator D much. This gives rise to the dip in Fig. 5(b). The order of magnitude of the term C_2 is larger than C_1 in the region $|\Delta_2|<G_1$ and this explains the behavior of ρ_{22} for $\gamma_2\neq\gamma_1$ (Fig. 4).

Physically, as the spontaneous decay rate from state $|1\rangle$ to state $|2\rangle$ increases more than the spontaneous decay rate from state $|1\rangle$ to state $|3\rangle$, more and more of the population gets settled in state $|2\rangle$. Only at the condition $\Delta_1=\Delta_2$ does the population get distributed equally (because of the condition $G_1=G_2$) between the states $|2\rangle$ and $|3\rangle$. This leads to the increase in sharpness of the dip with the increase in γ_2. If $\gamma_2<\gamma_1$, a peak is observed instead of a dip which is predicted from the Eq. (14).

For fields as low as 0.001 (scaled with respect to γ_1) the term with the second power of G_1 in Eq. (13) becomes negligible and hence the peak in C_1 disappears. However, for strong fields of the order of γ_1 this term becomes important and is responsible for the deep furrows on either side of the two-photon resonance condition as depicted in Fig. 6. But if the intensities of the fields are increased then the dip occurs only for very large γ_2 (Fig. 6). This is because the spontaneous emission from state $|1\rangle$ to state $|2\rangle$ has to be more effective than the field G_2 on the same transition to accumulate population on the level $|2\rangle$. The sharpness of the dip at $\Delta_1=\Delta_2=0$, indicating a fall in the population in level $|2\rangle$, is manifested only when more population is there on level $|2\rangle$ for detunings other than Δ_1. For smaller γ_2 the decrease in ρ_{22} at $\Delta_1=\Delta_2$ gets smoothed out due to the overall low population level for the values of detuning, Δ_2 not equal to zero. This dip in the population of the level $|2\rangle$ can be observed by studying the absorption out of the level $|2\rangle$ using a weak probe field as, for example, has been done in a different context in Ref. [8].

IV. CONCLUSIONS

In conclusion we have demonstrated that the phenomenon of CPT persists even at low light levels [14]. Futher, using a simple eigenvalue calculation and corroborating its prediction of the time scales involved by numerical integration of the atomic density-matrix equations for a Λ system, we have demonstrated how the evolution to the CPT state is dependent on the relative strengths of the fields and the spontaneous decays involved. We have shown that strong fields lead to the CPT state faster. Increasing the decay rates in the case of strong fields leads to CPT faster while in the case of weak fields it leads to a relatively slow evolution to CPT.

We have also demonstrated a sharp dip in the steady-state response of the Λ system when unequal spontaneous decay rates are assumed. The origin of the dip in the behavior of the population of the ground state is due to the trapping conditions at $\Delta_1=\Delta_2$.

Finally we mention that we have treated only a dilute medium. For a dense medium we have to account for the effect of the neighboring atoms, i.e., we have to include local-field corrections. This concept has been used in lasing without inversion to demonstrate enhancement of gain and enhancement of the index of refraction [10]. In a further publication we plan to study the dynamics of the atomic system in a dense medium where the near dipole-dipole effects become effective in the evolution to the CPT state.

[1] G. Alzetta, A. Gozzini, L. Moi, and G. Orriols, Nuovo Cimento B **36**, 5 (1976); G. Alzetta and L. Moi, *ibid.* **52**, 209 (1979).

[2] H. R. Gray, R. M. Whitley, and C. R. Stroud, Jr., Opt. Lett. **3**, 218 (1978); D. E. Murnick, M. S. Field, M. M. Burns, T. U. Kühl, and P. G. Pappas, in *Laser Spectroscopy*, 4th ed., edited by H. Walther and W. Rothe (Springer Verlag, Berlin, 1979), p. 195.

[3] G. Orriols, Nuovo Cimento A **53**, 1 (1979).

[4] F. T. Hioe and C. Carroll, Phys. Rev. A **37**, 3000 (1988); S. Swain, J. Phys. B **15**, 3405 (1982).

[5] P. M. Radmore and P. L. Knight, J. Phys. B **15**, 561 (1982); B. J. Dalton and P. L. Knight, *ibid.* **15**, 3997 (1982).

[6] G. S. Agarwal, Phys. Rev. Lett. **71**, 1351 (1993); see also M. Fleischhauer, *ibid.* **72**, 989 (1994).

[7] E. S. Fry, X. Li, D. Nikonov, G. G. Padmabandu, M. O. Scully, A. V. Smith, F. K. Tittel, C. Wang, S. R. Wilkinson, and S. Y. Zhu, Phys. Rev. Lett. **70**, 3235 (1993).

[8] S. Schiemann, A. Kuhn, S. Steuerwald, and K. Bergmann Phys. Rev. Lett. **71**, 3637 (1993).

[9] A. Imamoglu, J. E. Field, and S. E. Harris, Phys. Rev. Lett. **66**, 1154 (1991).

[10] J. P. Dowling and C. M. Bowden, Phys. Rev. Lett. **70**, 1421 (1993); A. S. Manka, J. P. Dowling, and C. M. Bowden, *ibid.* **73**, 1789 (1994).

[11] G. S. Agarwal and S. S. Jha, J. Phys. B **12**, 2655 (1979); A. S. Manka, H. M. Doss, L. M. Narducci, P. Ru, and G. L.

Oppo, Phys. Rev. A **43**, 3748 (1991).
[12] G. S. Agarwal, *Quantum Optics* (Springer Verlag, Berlin, 1974), Secs. 6, 7, and 18.
[13] This dynamical behavior should be observable by using the setup of Ref. [7] [E. S. Fry (private communication)].
[14] Y. Li and M. Xiao [Phys. Rev. A **51**, 4959 (1995)] have observed the persistence of quantum interference effects at low light levels using the transitions of ^{87}Rb.